Received: 24 October 2023 | Revised: 13 February 2024 | Accepted: 14 February 2024

DOI: 10.1002/jsp2.1318

RESEARCH ARTICLE

JOR Spine OPEN ACCESS

Comparative analysis of paraspinal muscle imbalance between idiopathic scoliosis and congenital scoliosis from the transcriptome aspect

Zhen Wang[1,2] | Junduo Zhao[1] | Haining Tan[3] | Yang Jiao[1] | Xin Chen[1] | Jianxiong Shen[1]

[1]Department of Orthopedics, Peking Union Medical College Hospital, Peking Union Medical College and Chinese Academy of Medical Sciences, Beijing, China

[2]Department of Orthopedics, The First Affiliated Hospital of Nanjing Medical University, Nanjing, China

[3]Department of Orthopedics, Beijing Friendship Hospital, Capital Medical University, Beijing, China

Correspondence
Jianxiong Shen, Department of Orthopedics, Peking Union Medical College Hospital, Peking Union Medical College and Chinese Academy of Medical Sciences, No. 1 Shuai Fu Yuan, Wang Fu Jing Street, Beijing 100730, China.
Email: sjxpumch@163.com

Funding information
National Natural Science Foundation of China, Grant/Award Numbers: 81772424, 81974354, 82230083

Abstract

Background: Previous studies have analyzed paraspinal muscle imbalance in idiopathic scoliosis (IS) with methods including imaging, histology and electromyography. However, whether paraspinal muscle imbalance is the cause or the consequence of spinal deformities in IS remains unclear. Comparison of paraspinal muscle imbalance between IS and congenital scoliosis (CS) may shed some light on the causality of paraspinal muscle imbalance and IS. This study aimed to elucidate the generality and individuality of paraspinal muscle imbalance between IS and CS from gene expression.

Methods: Five pairs of surgical-treated IS and CS patients were matched. Bilateral paraspinal muscles at the apex were collected for transcriptome sequencing. Differentially expressed genes (DEGs) between the convexity and concavity in both IS and CS were identified. Comparison of DEGs between IS and CS was conducted to discriminate IS-specific DEGs from DEGs shared by both IS and CS. Bioinformatics analysis was performed. The top 10 hub genes in the protein–protein interaction (PPI) network of IS-specific DEGs were validated by quantitative PCR (qPCR) in 10 pairs of IS and CS patients.

Results: A total of 370 DEGs were identified in IS, whereas 380 DEGs were identified in CS. Comparison of DEGs between IS and CS identified 59 DEGs shared by IS and CS, along with 311 DEGs specific for IS. These IS-specific DEGs were enriched in response to external stimulus and signaling receptor binding in GO terms and calcium signaling pathway in KEGG pathways. The top 10 hub genes in the PPI network of IS-specific DEGs include *BDKRB1*, *PRH1-TAS2R14*, *CNR2*, *NPY4R*, *HTR1E*, *CXCL3*, *ICAM1*, *ALB*, *ADIPOQ*, and *GCGR*. Among these hub genes, the asymmetrical expression of *PRH1-TAS2R14* and *ADIPOQ* in IS but not CS were validated by qPCR.

Conclusions: Transcriptomic differences in bilateral paraspinal muscles between the convexity and concavity in IS share few similarities with those in CS.

KEYWORDS
bioinformatic analysis, congenital scoliosis, differentially expressed genes, idiopathic scoliosis, paraspinal muscle imbalance

1 | INTRODUCTION

Idiopathic scoliosis (IS) is the most common type of scoliosis, occupying approximately 90% of all scoliotic patients.[1] In addition to appearance deformities, IS increases the risk of low back pain and reduces spinal mobility.[2–5] Moreover, the progression of thoracic curvature in IS may also cause cardiopulmonary dysfunction.[6,7] Currently, therapies targeting IS patients with a Cobb angle less than 25° are limited, partially due to the lack of clarity of the pathogenesis of the disease. Therefore, exploring the etiology and mechanism of IS may help to develop early interventions.

Imbalance of paraspinal muscles between the convexity and concavity is observed in both IS and congenital scoliosis (CS). Considering the existence of vertebral malformations, paraspinal muscle imbalance in CS is supposed to be secondary. Compared to CS, IS presents no prominent vertebral deformities. Therefore, it is speculated that IS may present primary muscle pathological changes. That is, paraspinal muscle imbalance in IS might be the comprehensive outcome of primary lesions and secondary changes. Distinguishing primary imbalance from secondary changes in bilateral paraspinal muscles may help to explore the pathogenesis of IS.

Previous studies have explored paraspinal muscle imbalance in IS with several methods. Ultrasound scan and magnetic resonance imaging demonstrated the discrepancy of bilateral paraspinal muscles in volume, thickness and cross-sectional area in IS,[8–10] whereas histopathological examinations revealed the differences in fiber distribution, the degree of fatty infiltration, the level of fibrosis and capillary count.[11,12] In addition, bilateral paraspinal muscles in IS also exhibit asymmetrical myoelectric activities.[13,14] However, the above studies can hardly determine the causality between paraspinal muscle imbalance and IS. To explore the precise role of paraspinal muscle imbalance in IS, Jiang and colleagues[15] applied next-generation sequencing and identified 40 DEGs, mainly enriched in Kyoto Encyclopedia of Genes and Genomes (KEGG) pathways, such as glycolysis/gluconeogenesis and adipocytokine signaling pathways. Similarly, Luo et al.[16] found 58 DEGs in paraspinal muscles between the concavity and convexity of IS, mainly enriched in the insulin signaling pathway and cyclic adenosine monophosphate (cAMP) signaling pathway. However, transcriptomic comparison of paraspinal muscle imbalance between IS and CS, which may help to exclude differentially expressed genes (DEGs) secondary to spinal deformities and identify IS-specific DEGs, is lacking.

This study aimed to compare paraspinal muscle imbalance between IS and CS from the aspect of transcriptome and sketch out the profile of IS-specific DEGs, thereby providing assistance to the understanding of the causality between paraspinal muscle imbalance and IS and the exploration of novel therapies targeting paraspinal muscle imbalance for IS.

2 | MATERIALS AND METHODS

2.1 | Participants

Surgically treated scoliotic patients in Peking Union Medical College Hospital from January 2022 to January 2024 were recruited. The inclusion criteria for the IS group were as follows: (1) thoracic curve as the major curve; and (2) primary posterior spinal fusion. The inclusion criteria for the CS group were as follows: (1) apex located between T5/6 and T11/12; (2) primary posterior spinal surgery; and (3) no neurological malformations, including syringomyelia, diastematomyelia, and tethered cord. After the matching of the two groups by age, sex and the location of the apical vertebra, five pairs of IS patients (Table 1) and CS patients (Table 2) were selected for transcriptome sequencing. Besides, 10 pairs of IS patients (Table 1) and CS patients (Table 2) were selected for the validation of gene expression. The process of this study was detailed in Figure 1.

This study was approved by the institutional review aboard of Peking Union Medical College Hospital (K4136) and performed according to the Helsinki Declaration. A written informed consent was obtained from adult patients or legal guardians.

2.2 | Sample processing

Multifidus on both the convexity and concavity at the apex were collected intraoperatively. Tissues were washed and dissected to the appropriate size. After immersion in RNA storage solution (Beyotime Biotechnology, Shanghai, China) at 4°C overnight, samples were transferred to −80°C for storage until use.

2.3 | RNA extraction, quantification, and qualification

Total RNA was extracted using the TRIzol method. RNA purity and concentration were detected using a NanoDrop 2000 spectrophotometer (Thermo Fisher, Waltham, MA, USA). The integrity and quantity were determined using an Agilent 4200 Bioanalyzer (Agilent, Santa Clara, CA, USA). Samples with an RNA concentration ≥40 ng/μL, amount ≥1 μg, and integrity number ≥6.0 were used for library construction.

2.4 | Library construction and mRNA-seq

mRNA was enriched using oligo (dT)-coated magnetic beads and broken into fragments. Templated by mRNA fragments, the first

TABLE 1 Detailed information for IS patients included in this study.

				Major curve				
No.	Age (years)	Sex	Classification	Range	Length (no. of vertebrae)	Cobb angle	Apex	Application
IS1	14	Male	Lenke 1AN	T6–T12	7	61	T9	RNA-seq
IS2	13	Female	Lenke 1A-	T5–T11	7	58	T8	RNA-seq
IS3	15	Female	Lenke 1A-	T7–L1	7	54	T10	RNA-seq
IS4	14	Female	Lenke 1A-	T5–T10	6	49	T9	RNA-seq
IS5	13	Female	Lenke 1AN	T5–T11	7	41	T8	RNA-seq
IS6	20	Male	Lenke 1A-	T5–L1	9	49	T8	qPCR
IS7	14	Female	Lenke 3CN	T6–T10	5	56	T9	qPCR
IS8	19	Female	Lenke 2AN	T6–T12	7	86	T9	qPCR
IS9	13	Female	Lenke 1AN	T5–T11	7	48	T8	qPCR
IS10	21	Female	Lenke 1AN	T3–T11	9	44	T7/8	qPCR
IS11	16	Male	Lenke 1AN	T5–T12	8	61	T9	qPCR
IS12	14	Female	Lenke 3CN	T6–T12	7	54	T9/10	qPCR
IS13	22	Female	Lenke 2AN	T6–L1	8	55	T9	qPCR
IS14	14	Male	Lenke 1AN	T5–T10	6	40	T8	qPCR
IS15	12	Female	Lenke 1BN	T5–T11	7	73	T8	qPCR

Abbreviations: IS, idiopathic scoliosis; L, lumbar vertebra; T, thoracic vertebra.

TABLE 2 Detailed information for CS patients included in this study.

				Major curve				
No.	Age (years)	Sex	Classification	Range	Length (no. of vertebrae)	Cobb angle	Apex	Application
CS1	13	Male	Formation failure	T9–T12	4	56	T10	RNA-seq
CS2	12	Female	Formation failure	T5–T10	6	51	T8	RNA-seq
CS3	15	Female	Segmentation failure	T10–T12	3	44	T11	RNA-seq
CS4	13	Female	Mixed type	T8–L2	7	67	T10	RNA-seq
CS5	12	Female	Segmentation failure	T5–L1	9	44	T8	RNA-seq
CS6	21	Male	Segmentation failure	T5–T10	6	106	T8	qPCR
CS7	14	Female	Segmentation failure	T6–L2	9	63	T10	qPCR
CS8	18	Female	Segmentation failure	T5–T12	8	52	T10	qPCR
CS9	13	Female	Segmentation failure	T6–T12	7	102	T9	qPCR
CS10	21	Female	Segmentation failure	T5–T9	5	70	T6/7	qPCR
CS11	15	Male	Formation failure	T5–T12	8	59	T10	qPCR
CS12	13	Female	Formation failure	T9–L1	5	67	T11	qPCR
CS13	23	Female	Formation failure	T5–T11	7	98	T9	qPCR
CS14	13	Male	Segmentation failure	T6–T12	7	81	T8/9	qPCR
CS15	13	Female	Segmentation failure	T5–T10	6	46	T7	qPCR

Abbreviations: CS, congenital scoliosis; L, lumbar vertebra; T, thoracic vertebra.

strand cDNA was reverse-transcribed using dNTPs, followed by the synthesis of the second strand cDNA. End repair was performed in double-strand cDNA. Then, the 3′ end was adenylated, followed by the ligation of sequencing adaptors. After purification via fragment filtering, cDNA was enriched by PCR amplification. The PCR product was further purified to obtain the RNA library.

After library construction, preliminary quantification of concentration was performed using a Qubit 3.0 fluorometer (Thermo Fisher, Waltham, MA, USA), followed by accurate quantification with a quantitative PCR (qPCR) method. Then, the samples were sequenced using the Illumina NovaSeq PE150 platform (Illumina, San Diego, CA, USA).

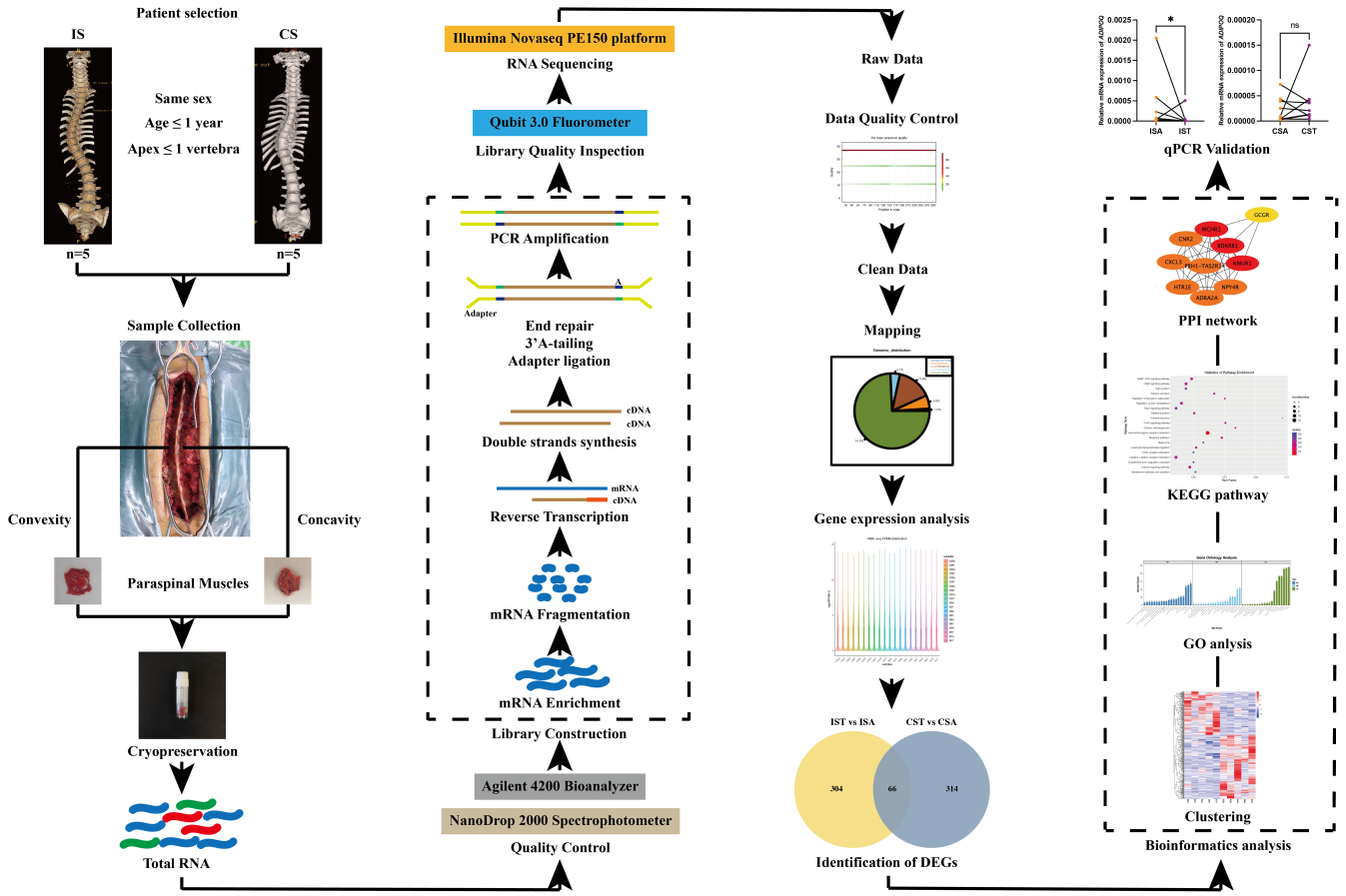

FIGURE 1 Workflow of this study. Generally, five pairs of idiopathic scoliosis (IS) patients and congenital scoliosis (CS) patients were matched by the standard of same sex, age difference within 1 year and apical region within 1 vertebra. Bilateral paraspinal muscles were collected intraoperatively and stored at −80°C. After extraction, total RNA was subjected to quality control. Then library construction was performed. Quality inspection of the library was conducted, followed by RNA sequencing with Illumina Novaseq 6000 platform at PE150 mode. Raw data were subjected to quality control to obtain clean data. Then clean data were mapped to human reference genome and qualitative and quantitative analysis of genes was performed. Differentially expressed genes (DEGs) between different groups were identified. Bioinformatic analyses of DEGs, including cluster analysis, GO functional enrichment, KEGG pathway enrichment and PPI analysis, was conducted. The expressions of the top 10 hub genes in the PPI network of IS-specific DEGs were validated with qPCR. CSA, paraspinal muscles on the concave side in congenital scoliosis; CST, paraspinal muscles on the convex side in congenital scoliosis; GO, gene ontology; ISA, paraspinal muscles on the concave side in idiopathic scoliosis; IST, paraspinal muscles on the convex side in idiopathic scoliosis; KEGG, Kyoto Encyclopedia of Genes and Genomes; PPI, protein–protein interaction; qPCR, quantitative polymerase chain reaction.

2.5 | Bioinformatic analysis

Raw data were subjected to quality control to obtain clean data. Then, paired-end clean reads were mapped onto the human reference genome (hg38). Identification of DEGs between groups was performed with the criteria of $|\log_2(\text{Fold Change})| > 1$ and P-value <0.05. Gene Ontology (GO) functional enrichment and KEGG pathway analysis of DEGs was performed. Visualization of protein–protein interactions (PPIs) was implemented using Cytoscape version 3.0.

2.6 | Comparison between groups

Paraspinal muscles on the convexity and concavity in IS were assigned to the IST group and the ISA group, respectively. Likewise, muscles on the convexity and concavity in CS were divided into the CST group and CSA group, respectively. Comparison between the IST and ISA groups was performed to explore DEGs in IS. Similarly, a comparison between the CST and CSA groups was performed to identify DEGs in CS. To discriminate DEGs in IS secondary to the deformities from those not, comparative analysis of DEGs between IS and CS was performed. DEGs in IS were divided into those shared by CS and those not. DEGs shared by IS and CS were further classified into two subgroups: those with the same difference between the convexity and concavity in IS and CS and those with the opposite difference in IS and CS. DEGs in IS sharing the same difference as CS were considered DEGs secondary to the deformities. DEGs in IS not shared by CS and DEGs in IS shared by CS but with the opposite difference were merged as IS-specific DEGs.

TABLE 3 Primer sequences for PCR analysis.

Genes	Sequence of primers (5′–3′)
BDKRB1	F: ATCAGCCAGGACCGCTACCG
	R: TTGGATGGATCGCAGCAGGAATG
PRH1-TAS2R14	F: GCCTGCTGGAACCTGCTGTATC
	R: GGCTTTGGTGCTGGCGTCTC
CNR2	F: GTCCCTGTTCATCGCCTTCCTC
	R: CCAACCTCACATCCAGCCTCATTC
NPY4R	F: CTCCATCCTCTCGCTCGTCCTC
	R: GACACAGGCAATGACCCAGATGAG
HTR1E	F: TCCACCAGCCTGCCAACTACC
	R: TCCACACTCAGCCACACCTCAC
CXCL3	F: GCGTCCGTGGTCACTGAACTG
	R: AGTGTGGCTATGACTTCGGTTTGG
ICAM1	F: GTCACCTATGGCAACGACTCCTTC
	R: AGTGTCTCCTGGCTCTGGTTCC
ALB	F: CCCAAGGCAACAAAAGAGCAACTG
	R: TCCTCGGCAAAGCAGGTCTCC
ADIPOQ	F: GACCAGGAAACCACGACTCAAGG
	R: AGGGGTGCCATCTCTGCCATC
GCGR	F: TGCTGGTGGCTGTCCTCTACTG
	R: GTTGCTGGTGTTCCGCTCCTC
18S	F: GGGGCCCGAAGCGTTTACTTTG
	R: CAAGAATTTCACCTCTAGCGGCGC

2.7 | Quantitative PCR analysis

Briefly, cDNA was synthesized using PrimeScript™ RT Master Mix (TaKaRa, Tokyo, Japan), according to the manufacturer's protocol. For the PCR amplification, 10 μL reaction volume containing 2 μL cDNA was prepared. Each cDNA sample was amplified using specific primers (Table 3). qPCR analysis was conducted in a QuantStudio™ 6 Flex System (Applied Biosystems, Foster city, CA, USA). Target gene expression levels were normalized to that of 18S. Relative expression levels were calculated using the $2^{-\Delta Ct}$ method. Paired t test or Wilcoxon matched-pairs signed rank test was performed to analyze gene expression differences in paraspinal muscles between the concavity and convexity in IS or CS.

3 | RESULTS

3.1 | Transcriptomic characteristics of paraspinal muscle imbalance in IS

A total of 370 DEGs were identified in IS, with 150 highly expressed in the IST group and 220 highly expressed in the ISA group (Figure 2A, B). DEGs in IS were enriched in GO terms, including response to external stimulus, system process and cell–cell signaling of the biological process (BP) domain (Figure 2C), signaling receptor binding and molecular function regulator of the molecular function (MF) domain (Figure 2D), along with plasma membrane and extracellular region of the cellular component (CC) domain (Figure 2E). KEGG analysis showed the enrichment of DEGs in various pathways, such as neuroactive ligand–receptor interaction, calcium signaling pathway and cAMP signaling pathway (Figure 2F). The top 10 hub genes in the PPI network of DEGs in IS included melanin concentrating hormone receptor 1 (*MCHR1*), neuromedin U receptor 1 (*NMUR1*), bradykinin receptor B1 (*BDKRB1*), neuropeptide Y receptor Y4 (*NPY4R*), adrenoceptor alpha 2A (*ADRA2A*), 5-hydroxytryptamine receptor 1E (*HTR1E*), C-X-C motif chemokine ligand 3 (*CXCL3*), proline rich protein HaeIII subfamily 1-taste 2 receptor member 14 readthrough (*PRH1-TAS2R14*), cannabinoid receptor 2 (*CNR2*), and glucagon receptor (*GCGR*) (Figure 2G).

3.2 | Transcriptomic characteristics of paraspinal muscle imbalance in CS

A total of 380 DEGs were identified in CS, with 235 highly expressed in the CST group and 145 highly expressed in the CSA group (Figure 3A, B). GO analysis showed the enrichment of DEGs in CS in multicellular organismal process and regulation of multicellular organismal process of the BP domain (Figure 3C), signaling receptor binding, receptor regulator activity and receptor ligand activity of the MF domain (Figure 3D), along with cell periphery and plasma membrane of the CC domain (Figure 3E). In addition, DEGs in IS were enriched in KEGG pathways, including neuroactive ligand–receptor interaction, tight junction, and the Rap1 signaling pathway (Figure 3F). The top 10 hub genes in the PPI network of DEGs in CS included *MCHR1*, *NMUR1*, cannabinoid receptor 1, neuropeptide Y receptor Y5, taste 2 receptor member 20, hydroxycarboxylic acid receptor 2, *ADRA2A*, C-X-C motif chemokine receptor 6, neuropeptide Y receptor Y1, and serum amyloid A1 (Figure 3G).

3.3 | Identification of IS-specific DEGs and DEGs with the same trend in IS and CS

As shown in Figure 4, the overlap of DEGs in IS and CS identified 66 DEGs shared by IS and CS. Among the 66 DEGs, 59 showing the same trend between the convexity and concavity in IS and CS were considered DEGs secondary to the deformities in IS. The remaining 7 displayed the opposite trend in IS and CS, and 304 DEGs in IS not shared by CS were defined as IS-specific DEGs.

3.4 | Bioinformatic analyses of DEGs with the same trend in IS and CS

Among the 59 DEGs with the same trend in IS and CS, 25 exhibited higher expression in the ISA group, whereas the remaining 34 were highly expressed in the IST group (Figure 5A). GO analysis revealed the enrichment of these DEGs in muscle system process and muscle contraction of the BP domain (Figure 5B), structural constituent of

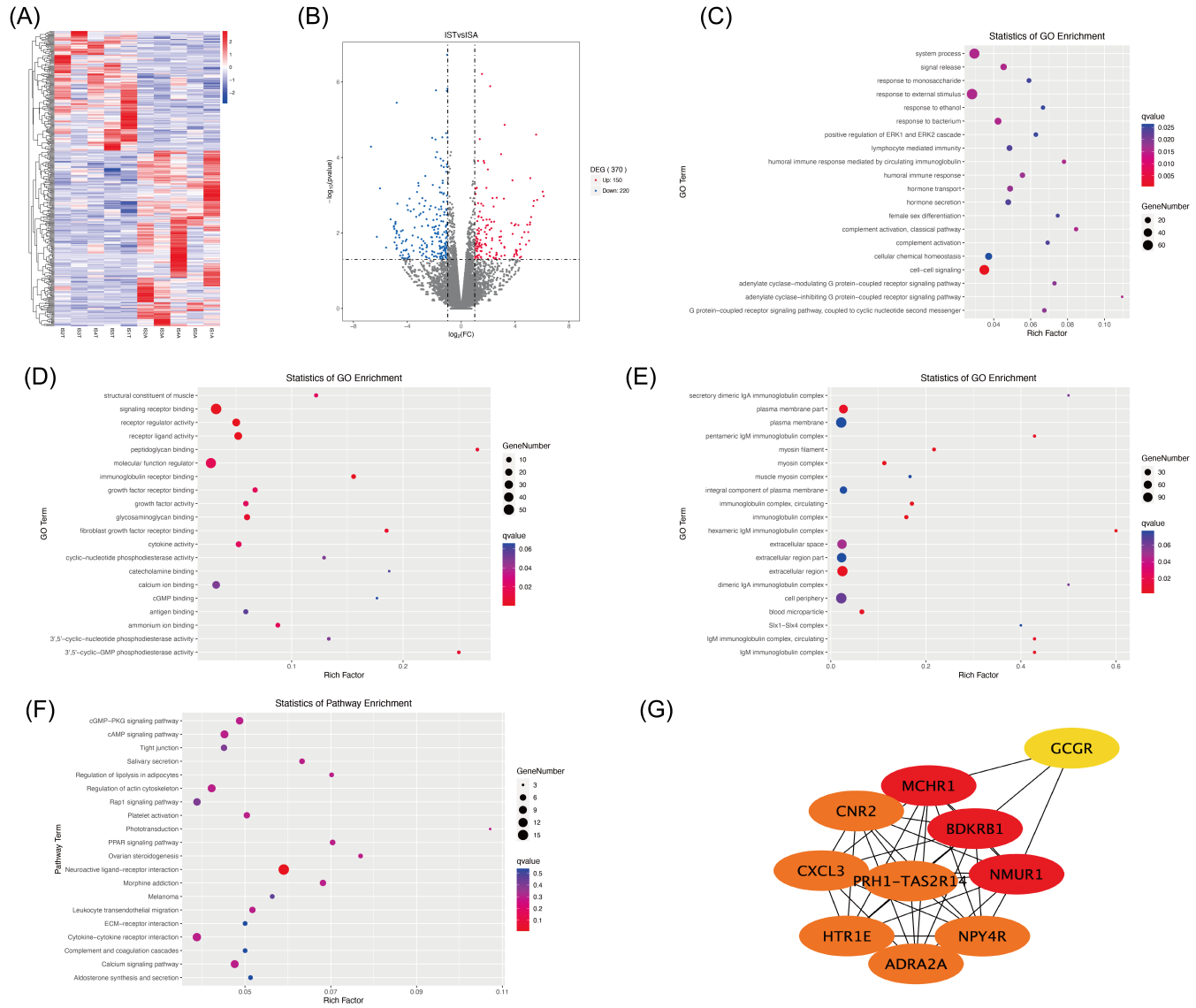

FIGURE 2 Transcriptomic analysis of paraspinal muscle imbalance in idiopathic scoliosis (IS). (A) Heatmap of Differentially expressed genes (DEGs) in paraspinal muscles between the convex and concave sides in IS. (B) Volcano plot of DEGs in bilateral paraspinal muscles of IS. (C) Enrichment of DEGs of IS in the category of biological process in GO terms. (D) Enrichment of DEGs of IS in the category of molecular function in GO terms. (E) Enrichment of DEGs of IS in the category of cellular component in GO terms. (F) Bubble plot of KEGG pathways in which DEGs in IS were enriched. (G) Top 10 hub genes among the PPI network of DEGs in IS. GO, Gene Ontology; ISA, paraspinal muscles on the concave side in idiopathic scoliosis; IST, paraspinal muscles on the convex side in idiopathic scoliosis; KEGG, Kyoto Encyclopedia of Genes and Genomes; PPI, protein–protein interaction.

muscle of the MF domain (Figure 5C), and myosin filament and myosin complex of the CC domain (Figure 5D). KEGG analysis indicated the enrichment of these DEGs in tight junction, neuroactive ligand–receptor interaction, and so forth. (Figure 5E). PPI analysis of these DEGs found six nodes and six edges (Figure 5F).

3.5 | Bioinformatic analyses of IS-specific DEGs

Among 311 IS-specific DEGs, 195 were highly expressed in the ISA group, whereas the remaining 116 were highly expressed in the IST group (Figure 6A). GO analysis showed the enrichment of IS-specific DEGs in response to external stimulus and cell–cell signaling of the BP domain (Figure 6B), signaling receptor binding and molecular function regulator of the MF domain (Figure 6C), along with the extracellular region and extracellular space of the CC domain (Figure 6D). In addition, these DEGs were enriched in KEGG pathways, such as neuroactive ligand–receptor interaction and calcium signaling pathway (Figure 6E). The top 10 hub genes in the PPI network of IS-specific DEGs included *BDKRB1*, *PRH1-TAS2R14*, *CNR2*, *NPY4R*, *HTR1E*, *CXCL3*, intercellular adhesion molecule 1 (*ICAM1*), albumin (*ALB*), adiponectin (*ADIPOQ*), and *GCGR* (Figure 6F).

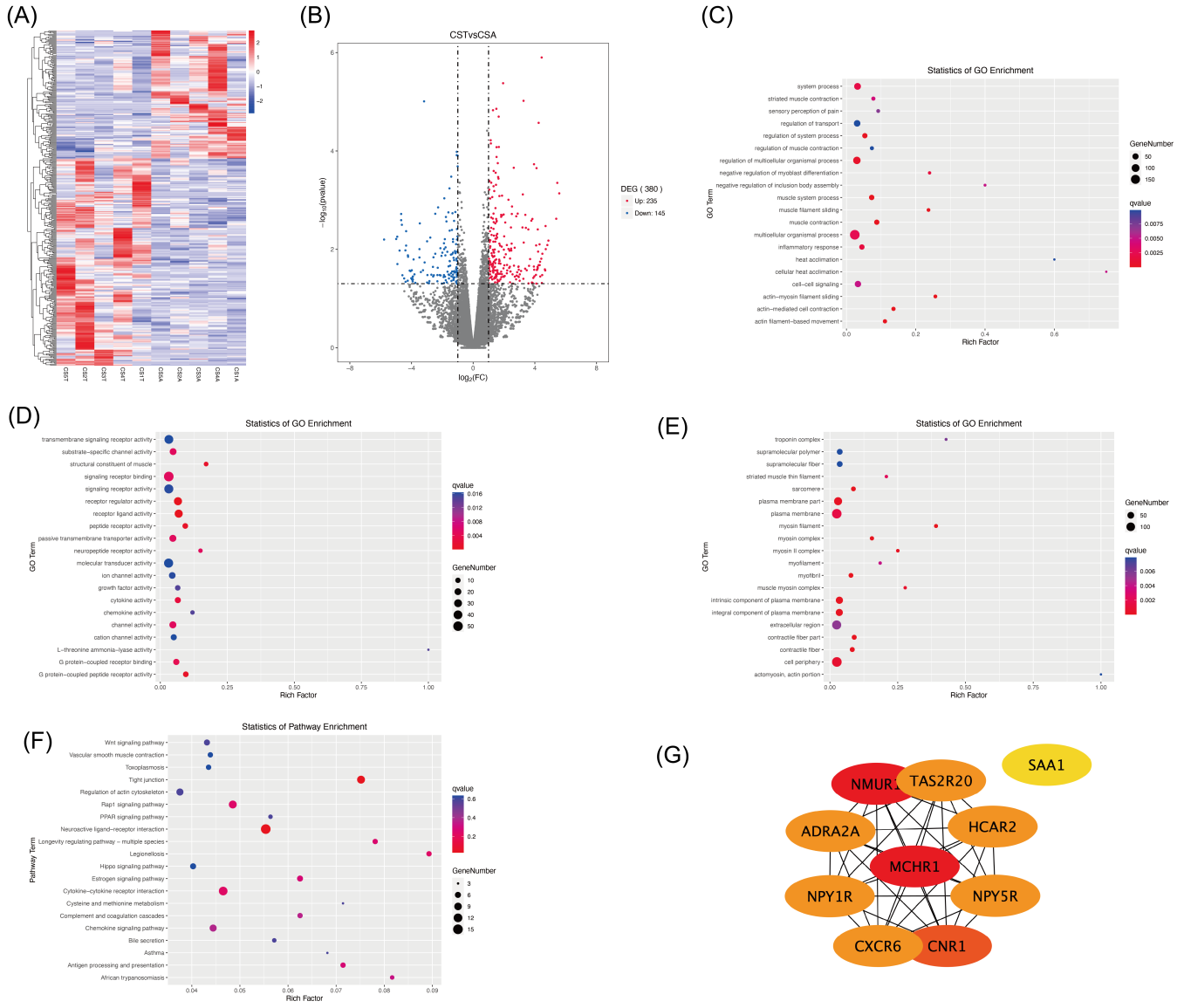

FIGURE 3 Transcriptomic analysis of paraspinal muscle imbalance in congenital scoliosis (CS). (A) Heatmap of differentially expressed genes (DEGs) in paraspinal muscles between the convex and concave sides in CS. (B) Volcano plot of DEGs in the bilateral paraspinal muscles of CS. (C) Enrichment of DEGs of CS in the category of biological process in GO terms. (D) Enrichment of DEGs of CS in the category of molecular function in GO terms. (E) Enrichment of DEGs of CS in the category of cellular component in GO terms. (F) Bubble plot of KEGG pathways in which DEGs in CS were enriched. (G) Top 10 hub genes among the PPI network of DEGs in CS. CSA, paraspinal muscles on the concave side in congenital scoliosis; CST, paraspinal muscles on the convex side in congenital scoliosis; GO, Gene Ontology; KEGG, Kyoto Encyclopedia of Genes and Genomes; PPI, protein–protein interaction.

3.6 | Validation of the expressions of IS-specific DEGs

Validation of the expressions of the top 10 hub genes in the PPI network of IS-specific DEGs demonstrated no significant differences in paraspinal muscles between the concavity and convexity in both IS and CS regarding *BDKRB1*, *CNR2*, *NPY4R*, *HTR1E*, *CXCL3*, *ICAM1*, *ALB* and *GCGR* (Figure 7A, C–H, J). Asymmetrical mRNA levels of *PRH1-TAS2R14* and *ADIPOQ* were observed in IS with higher expressions in paraspinal muscles on the concavity, whereas no statistical differences regarding the expressions of *PRH1-TAS2R14* and *ADIPOQ* in bilateral paraspinal muscles of CS were observed (Figure 7B, I).

4 | DISCUSSION

This study described the transcriptomic characteristics of paraspinal muscle imbalance in IS and CS and verified the great difference in the transcriptome for paraspinal muscle imbalance between IS and CS. In addition, through the comparison of DEGs between IS and CS, we

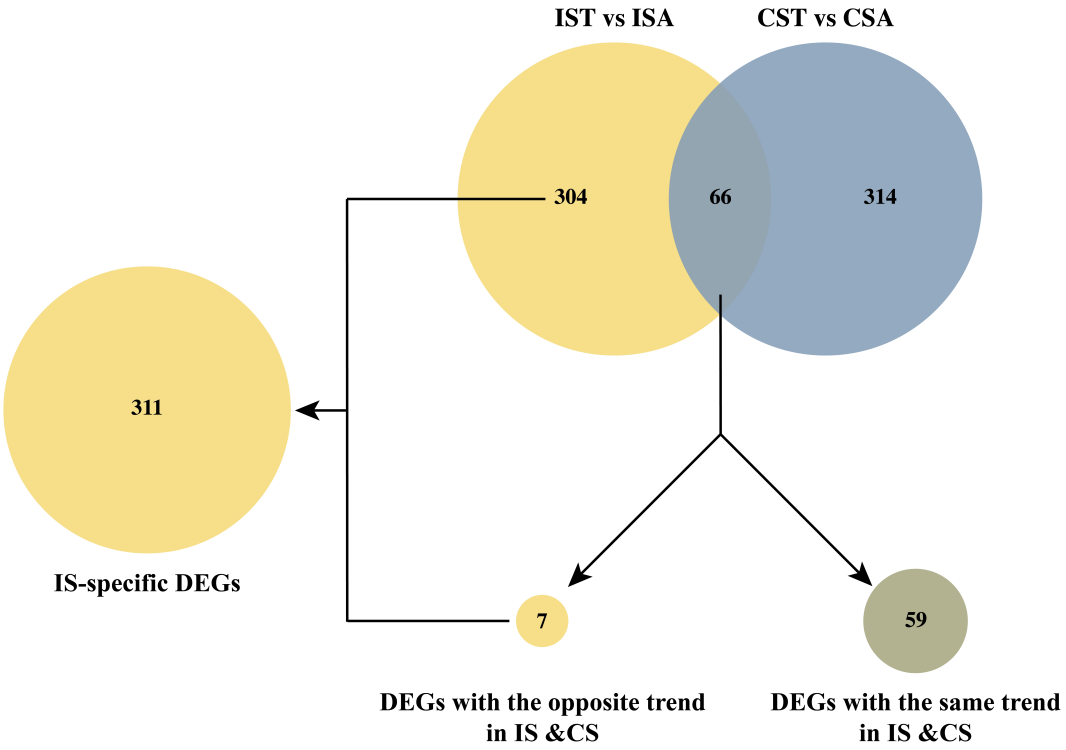

FIGURE 4 Identification of idiopathic scoliosis (IS)-specific differentially expressed genes (DEGs). Venn diagram showing the overlap of 66 DEGs in IS and congenital scoliosis (CS). These genes were classified into two groups: DEGs with the same trend shared by IS and CS (59) and DEGs with the opposite trend shared by IS and CS (7). DEGs with the opposite trend shared by IS and CS and DEGs in IS not shared by CS were considered IS-specific DEGs (311). CSA, paraspinal muscles on the concave side in congenital scoliosis; CST, paraspinal muscles on the convex side in congenital scoliosis; ISA, paraspinal muscles on the concave side in idiopathic scoliosis; IST, paraspinal muscles on the convex side in idiopathic scoliosis.

identified the profile of IS-specific DEGs for paraspinal muscle imbalance in IS.

Genome-wide associated studies have identified dozens of susceptible genes for IS in the last decade. Among these genes, several are differentially expressed in bilateral paraspinal muscles of IS, including ladybird homeobox protein homolog 1, adhesion G protein-coupled receptor G6, paired box 1, paired box 3, TRAF2 and NCK interacting kinase, Meis homeobox 1, *β-catenin*, and suppressor of cytokine signaling 3.[17–21] However, the above studies failed to provide global differences in bilateral paraspinal muscles from the aspect of omics. Herein, we applied transcriptomic sequencing and identified 370 DEGs in bilateral paraspinal muscles of IS, much greater than the number of DEGs in previous studies.[15,16] The great differences regarding the number of DEGs between this study and previous studies may be attributed to the different filters. Among the 58 DEGs identified by Luo and colleagues,[16] *Tent5a* participates in the progression of IS through inhibiting the proliferation and migration of myoblasts and the maturation of type I myofibers. However, whether these gene expression differences in the bilateral paraspinal muscles of IS are primary or secondary remains unclear. To rule out differential genes secondary to the deformities, Jiang and colleagues[15] introduced age-matched CS patients as the control and identified 2 critical DEGs specific for IS—*H19* and *ADIPOQ*. Notably, they did not take parameters, including sex and the location of the apical vertebra, into account. In addition, intraspinal anomalies, which may interfere with the development and function of paraspinal muscles, should be ruled out in the CS group. In this study, CS patients without intraspinal abnormalities were selected as the control group. Age and sex were matched between the IS and CS groups. Besides, no significant differences were observed regarding major curve length and Cobb angle between the IS group and the CS group. Transcriptome sequencing showed that the number of DEGs in IS was comparable to that in CS. However, approximately 60% of DEGs in IS were highly expressed on the concavity, whereas 60% of DEGs in CS exhibited higher expressions on the convexity. GO analysis showed that only 15 of the 106 BP terms in which DEGs in IS were enriched were shared by CS. In addition, 9 of the 17 MF terms and 6 of the 12 CC terms in which DEGs in IS were enriched were shared by CS. Regarding KEGG pathways, 5 of the 17 pathways in which DEGs in IS were enriched were shared by CS. Among the top 10 hub genes in the PPI network of DEGs in IS, only 3 were shared by CS. These data suggest significant differences between DEGs in IS and those in CS regarding the type, distribution, function and interactions.

Through the comparison of IS and CS, we divided DEGs in IS into DEGs shared by IS and CS and IS-specific DEGs. Of note, DEGs shared by IS and CS account for only 16% of DEGs in IS, whereas the remaining 84% were IS-specific DEGs. Functional analysis showed the enrichment of IS-specific DEGs in various terms associated with

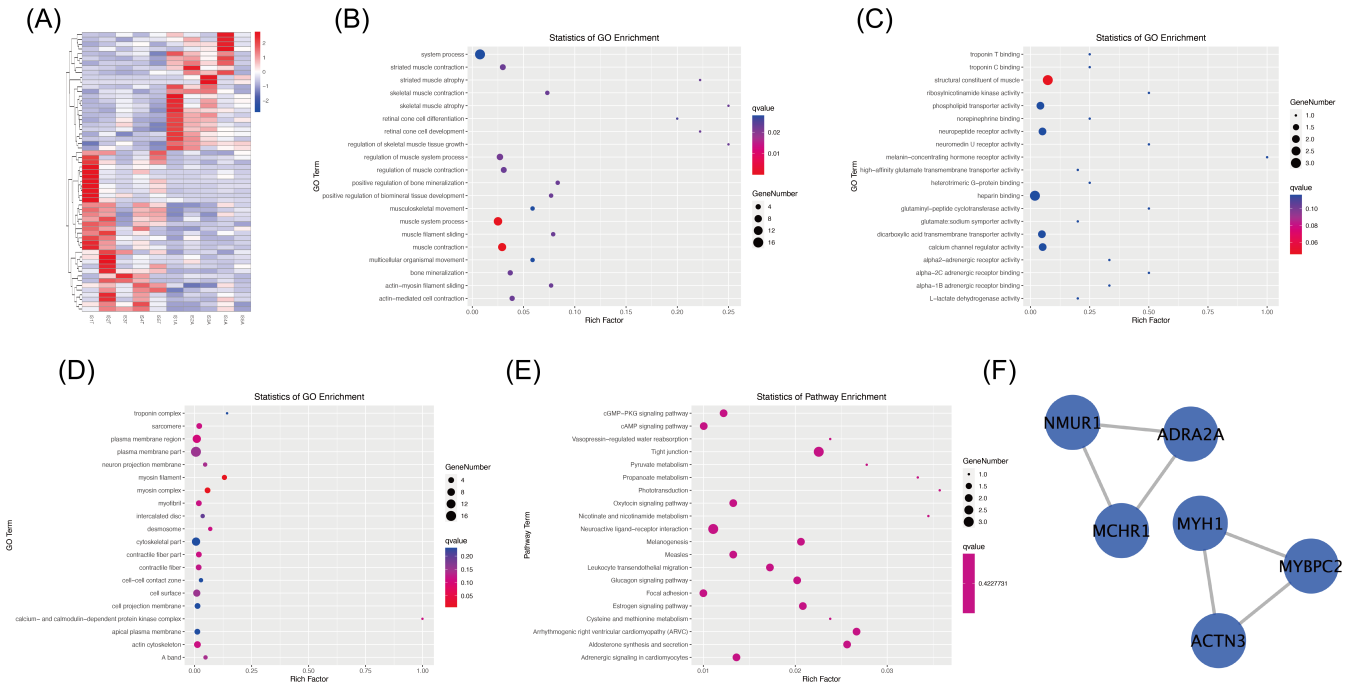

FIGURE 5 Bioinformatic analysis of differentially expressed genes (DEGs) with the same trend shared by idiopathic scoliosis (IS) and congenital scoliosis (CS). (A) Heatmap of DEGs with the same trend shared by IS and CS. (B) Enrichment of DEGs with the same trend shared by IS and CS in the category of biological process in GO terms. (C) Enrichment of DEGs with the same trend shared by IS and CS in the category of molecular function in GO terms. (D) Enrichment of DEGs with the same trend shared by IS and CS in the category of cellular component in GO terms. (E) Bubble plot of KEGG pathways in which DEGs with the same trend shared by IS and CS were enriched. (F) PPI network of DEGs with the same trend shared by IS and CS. GO, Gene Ontology; ISA, paraspinal muscles on the concave side in idiopathic scoliosis; IST, paraspinal muscles on the convex side in idiopathic scoliosis; KEGG, Kyoto Encyclopedia of Genes and Genomes; PPI, protein–protein interaction.

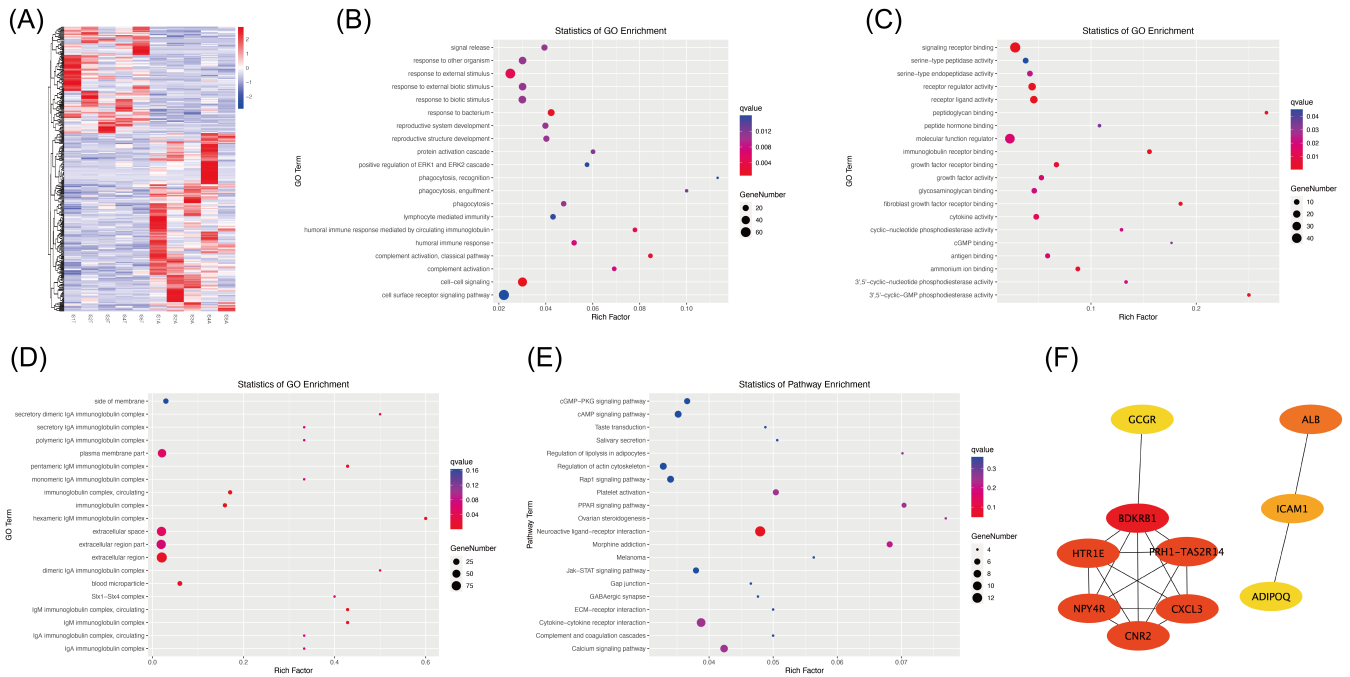

FIGURE 6 Bioinformatic analysis of idiopathic scoliosis (IS)-specific differentially expressed genes (DEGs). (A) Heatmap of IS-specific DEGs. (B) Enrichment of IS-specific DEGs in the category of biological process in GO terms. (C) Enrichment of IS-specific DEGs in the category of molecular function in GO terms. (D) Enrichment of IS-specific DEGs in the category of cellular component in GO terms. (E) Bubble plot of KEGG pathways in which IS-specific DEGs were enriched. (F) Top 10 hub genes among the PPI network of IS-specific DEGs. CS, congenital scoliosis; GO, Gene Ontology; ISA, paraspinal muscles on the concave side in idiopathic scoliosis; IST, paraspinal muscles on the convex side in idiopathic scoliosis; KEGG, Kyoto Encyclopedia of Genes and Genomes; PPI, protein–protein interaction.

cAMP signaling pathway, such as adenylate cyclase-inhibiting G protein-coupled receptor signaling pathway, cyclic-nucleotide-mediated signaling, adenylate cyclase-modulating G protein-coupled receptor signaling pathway, cAMP-mediated signaling of the BP domain. Besides, IS-specific DEGs were also enriched in terms associated with cyclic guanosine monophosphate (cGMP), which serves as an antagonist of cAMP, such as 3′,5′-cGMP phosphodiesterase activity and cGMP binding of the MF domain. KEGG analysis also indicated the enrichment of IS-specific DEGs in cAMP signaling pathway and cGMP-protein kinase G (PKG) signaling pathway. As is known, cAMP signaling pathway mediates energy utilization and muscle contraction through the regulation of glycogenolysis and sarcoplasmic calcium kinetics. In skeletal muscles, the activation of the cAMP signaling pathway may increase muscle volume and promote the conversion of type II myofibers to type I myofibers.[22] Noteworthily, DEGs shared by IS and CS were also enriched in cAMP pathway and cGMP-PKG pathway. Therefore, we suggest that

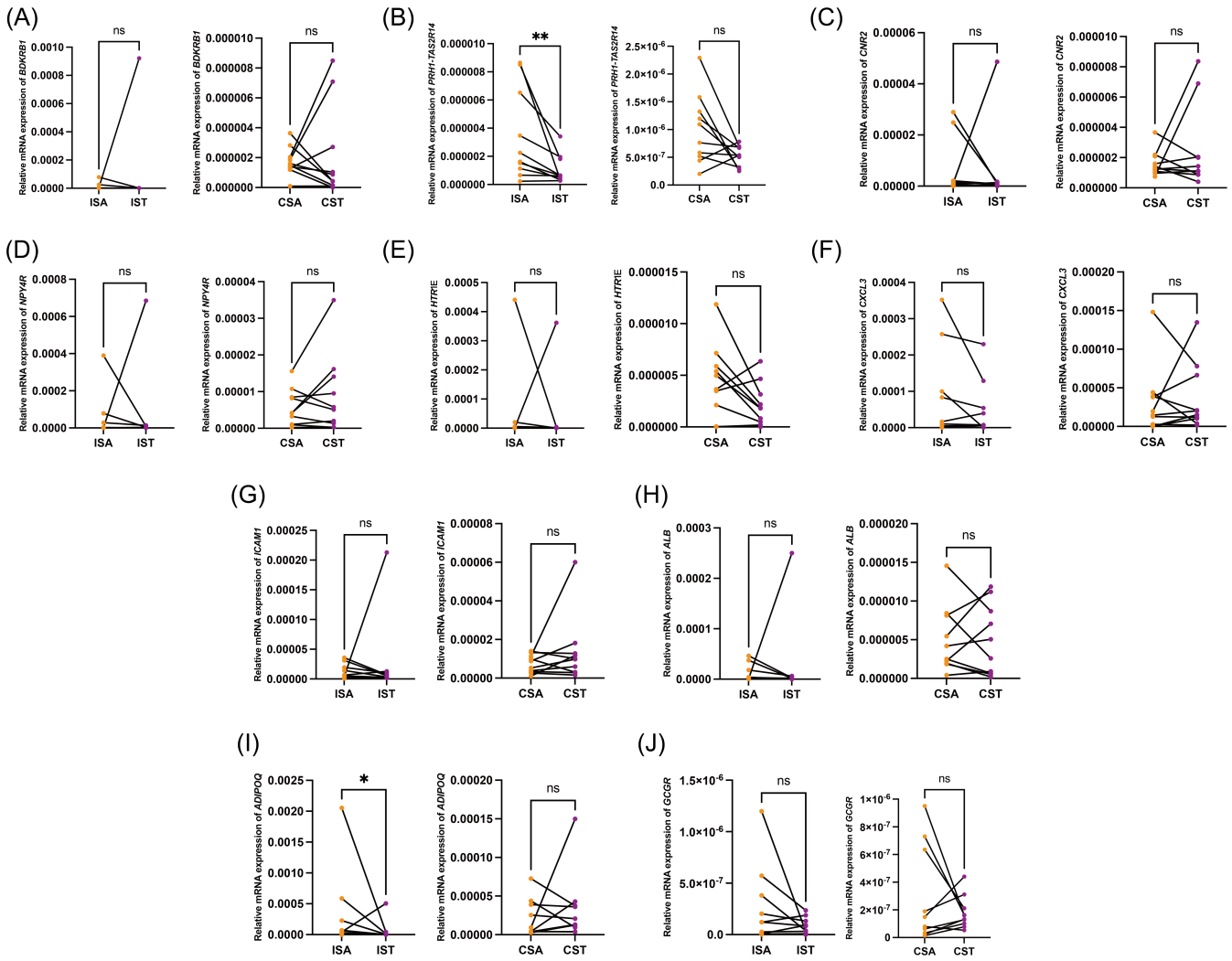

FIGURE 7 Validation of the expressions of idiopathic scoliosis (IS)-specific differentially expressed genes (DEGs) with qPCR. (A) Differences regarding the mRNA expression of *BDKRB1* in paraspinal muscles between the concavity and convexity of IS and congenital scoliosis (CS). (B) Differences regarding the mRNA expression of *PRH1-TAS2R14* in paraspinal muscles between the concavity and convexity of IS and CS. (C) Differences regarding the mRNA expression of *CNR2* in paraspinal muscles between the concavity and convexity of IS and CS. (D) Differences regarding the mRNA expression of *NPY4R* in paraspinal muscles between the concavity and convexity of IS and CS. (E) Differences regarding the mRNA expression of *HTR1E* in paraspinal muscles between the concavity and convexity of IS and CS. (F) Differences regarding the mRNA expression of *CXCL3* in paraspinal muscles between the concavity and convexity of IS and CS. (G) Differences regarding the mRNA expression of *ICAM1* in paraspinal muscles between the concavity and convexity of IS and CS. (H) Differences regarding the mRNA expression of *ALB* in paraspinal muscles between the concavity and convexity of IS and CS. (I) Differences regarding the mRNA expression of *ADIPOQ* in paraspinal muscles between the concavity and convexity of IS and CS. (J) Differences regarding the mRNA expression of *GCGR* in paraspinal muscles between the concavity and convexity of IS and CS. (^{ns}P >0.05 between groups; $^{*}P$ < 0.05 between groups; $^{**}P$ < 0.01 between groups). CSA, paraspinal muscles on the concave side in congenital scoliosis; CST, paraspinal muscles on the convex side in congenital scoliosis; ISA, paraspinal muscles on the concave side in idiopathic scoliosis; IST, paraspinal muscles on the convex side in idiopathic scoliosis.

metabolic imbalance and the asymmetrical distribution of myofibers in bilateral paraspinal muscles of IS might be the comprehensive results of primary lesions and secondary changes. Previous study revealed an upregulation of calcium levels in the paraspinal muscles of IS. In addition, the calcium level in muscles on the convexity is higher than that on the concavity.[23] In this study, IS-specific DEGs were also enriched in the calcium signaling pathway. Considering the importance of intracellular calcium homeostasis for muscle contraction and the maintenance of muscle tone, we assumed that the imbalance in calcium ion levels and asymmetrical activation of the calcium signaling pathway in bilateral paraspinal muscles may participate in the pathogenesis of IS.[24] Patients with IS were reported to have decreased serum estrogen levels.[25,26] In addition, polymorphisms in estrogen receptor 1 (ESR1) and estrogen receptor 2 (ESR2) are associated with susceptibility to and progression of IS.[27–31] An asymmetrical distribution of ESR1 and ESR2 in the bilateral paraspinal muscles was reported.[32,33] Recently, Shao and colleagues demonstrated that disrupted ESR1 signaling in muscle progenitor cells at the concavity may be responsible for the progression of IS.[34] However, in this study, DEGs in bilateral paraspinal muscles shared by IS and CS, instead of IS-specific genes, were enriched in the estrogen signaling pathway. Accordingly, we speculated that asymmetrical activation of the estrogen signaling pathway tends to be secondary to the deformities. Validation of gene expressions with qPCR demonstrated that 8 of the top 10 hub genes in the PPI network of IS-specific genes showed no statistical differences in bilateral paraspinal muscles of IS, indicating the elusive genetic factors for IS. Besides, the low expressions of target genes in comparison to the reference gene may to some degree overshadow the differences between the concavity and convexity in paraspinal muscles of IS. Consistent with a previous study, asymmetrical expression of *ADIPOQ* in IS instead of CS was also validated in our cohort.[15] As is known, *ADIPOQ* reduces the content of intramyocellular lipid, increases type II myofiber area, attenuates inflammation and promotes myogenesis.[35–37] Therefore, asymmetrical expression of *ADIPOQ* may mediate paraspinal muscle imbalance in development and function, thus contributing to IS. In addition to *ADIPOQ*, asymmetric expression of *PRH1-TAS2R14* in bilateral paraspinal muscles of IS was also confirmed. As a readthrough transcript, *PRH1-TAS2R14* encodes a fusion protein that shares sequence identity with each individual gene product. Until now few literatures report the function of *PRH1-TAS2R14* in skeletal muscles. In that case, the precise role of *PRH1-TAS2R14* in IS remains to be clarified.

The limitations of this study deserve attention. First, the sample size was relatively small, partially due to the low incidence of CS. Second, as a descriptive study, this study only provides the landscape of IS-specific DEGs. In the future, further study with large samples is required to validate the expression of these DEGs and explore the role of these genes in the pathogenesis of IS.

5 | CONCLUSIONS

Both IS and CS exhibit transcriptomic imbalance in paraspinal muscles between the convexity and concavity. However, the transcriptome profile for paraspinal muscle imbalance differed greatly between IS and CS, suggesting different causalities between paraspinal muscle imbalance and spinal deformities in IS and CS. In addition to transcriptomic imbalance secondary to spinal deformities, there are some primary imbalances in the transcriptome in IS, which may account for the pathogenesis of IS.

AUTHOR CONTRIBUTIONS

ZW was involved in data curation, formal analysis, visualization and writing–original draft; JS contributed to conceptualization, project administration, funding acquisition and is responsible; JZ, HT, YJ, and XC contributed to writing–review and editing. All authors have read and approved the final version of the manuscript.

ACKNOWLEDGMENTS

We appreciate all participants for their contributions to this work. Mr. Zhen Wang thank Ms. Renrui Zou from Nanjing Medical University for her support in the implementation of this study.

CONFLICT OF INTEREST STATEMENT

The authors declare no conflicts of interest.

DATA AVAILABILITY STATEMENT

RNA sequencing data for this study have been submitted to the GEO database under the accession number GSE254300.

ORCID

Zhen Wang https://orcid.org/0000-0002-6997-8264

REFERENCES

1. Marya S, Tambe AD, Millner PA, Tsirikos AI. Adolescent idiopathic scoliosis: a review of aetiological theories of a multifactorial disease. *Bone Joint J*. 2022;104-B(8):915-921.
2. Makino T, Kaito T, Kashii M, Iwasaki M, Yoshikawa H. Low back pain and patient-reported QOL outcomes in patients with adolescent idiopathic scoliosis without corrective surgery. *Springerplus*. 2015;4:397.
3. Theroux J, Le May S, Hebert JJ, Labelle H. Back pain prevalence is associated with curve-type and severity in adolescents with idiopathic scoliosis: a cross-sectional study. *Spine*. 2017;42(15):E914-E919.
4. Calvo-Munoz I, Gomez-Conesa A, Sanchez-Meca J. Prevalence of low back pain in children and adolescents: a meta-analysis. *BMC Pediatr*. 2013;13:14.
5. Eyvazov K, Samartzis D, Cheung JP. The association of lumbar curve magnitude and spinal range of motion in adolescent idiopathic scoliosis: a cross-sectional study. *BMC Musculoskelet Disord*. 2017;18(1):51.
6. Kan MMP, Negrini S, Di Felice F, et al. Is impaired lung function related to spinal deformities in patients with adolescent idiopathic scoliosis? A systematic review and meta-analysis-SOSORT 2019 award paper. *Eur Spine J*. 2023;32(1):118-139.
7. Li S, Yang J, Li Y, et al. Right ventricular function impaired in children and adolescents with severe idiopathic scoliosis. *Scoliosis*. 2013;8(1):1.
8. Zapata KA, Wang-Price SS, Sucato DJ, Dempsey-Robertson M. Ultrasonographic measurements of paraspinal muscle thickness in adolescent idiopathic scoliosis: a comparison and reliability study. *Pediatr Phys Ther*. 2015;27(2):119-125.
9. Kennelly KP, Stokes MJ. Pattern of asymmetry of paraspinal muscle size in adolescent idiopathic scoliosis examined by real-time ultrasound imaging. A preliminary study. *Spine*. 1993;18(7):913-917.

10. Xu JJ, Zhu XL, Li T, et al. Assessment of the cross-sectional areas of the psoas major in patients with adolescent idiopathic scoliosis before skeletal maturity. *Acta Radiol*. 2021;62(5):639-645.
11. Zetterberg C, Aniansson A, Grimby G. Morphology of the paravertebral muscles in adolescent idiopathic scoliosis. *Spine*. 1983;8(5):457-462.
12. Wajchenberg M, Martins DE, Luciano RP, et al. Histochemical analysis of paraspinal rotator muscles from patients with adolescent idiopathic scoliosis: a cross-sectional study. *Medicine (Baltimore)*. 2015;94(8):e598.
13. Shimode M, Ryouji A, Kozo N. Asymmetry of premotor time in the back muscles of adolescent idiopathic scoliosis. *Spine*. 2003;28(22):2535-2539.
14. Ng PTT, Claus A, Izatt MT, Pivonka P, Tucker K. Is spinal neuromuscular function asymmetrical in adolescents with idiopathic scoliosis compared to those without scoliosis? A narrative review of surface EMG studies. *J Electromyogr Kinesiol*. 2022;63:102640.
15. Jiang H, Yang F, Lin T, et al. Asymmetric expression of H19 and ADIPOQ in concave/convex paravertebral muscles is associated with severe adolescent idiopathic scoliosis. *Mol Med*. 2018;24(1):48.
16. Luo M, Yang H, Wu D, You X, Huang S, Song Y. Tent5a modulates muscle fiber formation in adolescent idiopathic scoliosis via maintenance of myogenin expression. *Cell Prolif*. 2022;55(3):e13183.
17. Zhu Z, Xu L, Leung-Sang Tang N, et al. Genome-wide association study identifies novel susceptible loci and highlights Wnt/beta-catenin pathway in the development of adolescent idiopathic scoliosis. *Hum Mol Genet*. 2017;26(8):1577-1583.
18. Wang Y, Feng Z, Cheng KL, et al. Role of differentially expressed LBX1 in adolescent idiopathic scoliosis (AIS) paraspinal muscle phenotypes and muscle-bone crosstalk through modulating myoblasts. *Stud Health Technol Inform*. 2021;280:14-17.
19. Xu L, Sheng F, Xia C, et al. Genetic variant of PAX1 gene is functionally associated with adolescent idiopathic scoliosis in the Chinese population. *Spine*. 2018;43(7):492-496.
20. Xu E, Lin T, Jiang H, et al. Asymmetric expression of GPR126 in the convex/concave side of the spine is associated with spinal skeletal malformation in adolescent idiopathic scoliosis population. *Eur Spine J*. 2019;28(9):1977-1986.
21. Xu L, Dai Z, Xia C, et al. Asymmetric expression of Wnt/B-catenin pathway in AIS: primary or secondary to the curve? *Spine*. 2020;45(12):E677-E683.
22. Chen M, Feng HZ, Gupta D, et al. G(s)alpha deficiency in skeletal muscle leads to reduced muscle mass, fiber-type switching, and glucose intolerance without insulin resistance or deficiency. *Am J Physiol Cell Physiol*. 2009;296(4):C930-C940.
23. Yarom R, Robin GC, Gorodetsky R. X-ray fluorescence analysis of muscles in scoliosis. *Spine*. 1978;3(2):142-145.
24. Tu MK, Levin JB, Hamilton AM, Borodinsky LN. Calcium signaling in skeletal muscle development, maintenance and regeneration. *Cell Calcium*. 2016;59(2–3):91-97.
25. Kulis A, Zarzycki D, Jaskiewicz J. Concentration of estradiol in girls with idiophatic scoliosis. *Ortop Traumatol Rehabil*. 2006;8(4):455-459.
26. Kulis A, Gozdzialska A, Drag J, et al. Participation of sex hormones in multifactorial pathogenesis of adolescent idiopathic scoliosis. *Int Orthop*. 2015;39(6):1227-1236.
27. Inoue M, Minami S, Nakata Y, et al. Association between estrogen receptor gene polymorphisms and curve severity of idiopathic scoliosis. *Spine*. 2002;27(21):2357-2362.
28. Wu J, Qiu Y, Zhang L, Sun Q, Qiu X, He Y. Association of estrogen receptor gene polymorphisms with susceptibility to adolescent idiopathic scoliosis. *Spine*. 2006;31(10):1131-1136.
29. Nikolova S, Yablanski V, Vlaev E, Stokov L, Savov A, Kremensky I. Association between estrogen receptor alpha gene polymorphisms and susceptibility to idiopathic scoliosis in Bulgarian patients: a case-control study. *Open Access Maced J Med Sci*. 2015;3(2):278-282.
30. Zhang HQ, Lu SJ, Tang MX, et al. Association of estrogen receptor beta gene polymorphisms with susceptibility to adolescent idiopathic scoliosis. *Spine*. 2009;34(8):760-764.
31. Kotwicki T, Janusz P, Andrusiewicz M, Chmielewska M, Kotwicka M. Estrogen receptor 2 gene polymorphism in idiopathic scoliosis. *Spine*. 2014;39(26):E1599-E1607.
32. Kudo D, Miyakoshi N, Hongo M, et al. Nerve growth factor and estrogen receptor mRNA expression in paravertebral muscles of patients with adolescent idiopathic scoliosis: a preliminary study. *Spine Deform*. 2015;3(2):122-127.
33. Rusin B, Kotwicki T, Głodek A, Andrusiewicz M, Urbaniak P, Kotwicka M. Estrogen receptor 2 expression in back muscles of girls with idiopathic scoliosis – relation to radiological parameters. *Stud Health Technol Inform*. 2012;176:59-62.
34. Shao X, Fu X, Yang J, et al. The asymmetrical ESR1 signaling in muscle progenitor cells determines the progression of adolescent idiopathic scoliosis. *Cell Discov*. 2023;9(1):44.
35. Krause MP, Liu Y, Vu V, et al. Adiponectin is expressed by skeletal muscle fibers and influences muscle phenotype and function. *Am J Physiol Cell Physiol*. 2008;295(1):C203-C212.
36. Jortay J, Senou M, Abou-Samra M, et al. Adiponectin and skeletal muscle: pathophysiological implications in metabolic stress. *Am J Pathol*. 2012;181(1):245-256.
37. Krause MP, Milne KJ, Hawke TJ. Adiponectin-consideration for its role in skeletal muscle health. *Int J Mol Sci*. 2019;20(7):1528.

How to cite this article: Wang Z, Zhao J, Tan H, Jiao Y, Chen X, Shen J. Comparative analysis of paraspinal muscle imbalance between idiopathic scoliosis and congenital scoliosis from the transcriptome aspect. *JOR Spine*. 2024;7(1):e1318. doi:10.1002/jsp2.1318